Effect of convective and radiative heat transfer in evaporative losses during beef cooling

A. Urquiola[1,*], P. Galione[1], P. Curto-Risso[1]

Abstract

In the present work a numerical analysis is presented to identify the separate effect of cooling by radiation and convection, in evaporative meat weight loss during beef carcass cooling process. A transient heat and mass transfer model is proposed using a 3D beef side geometry. Water activity variations are incorporated in the model. Convective coefficients are obtained from correlations by considering buoyancy effect due to temperature and vapor concentration gradients, and forced air flow. For the purpose of model water mass diffusion into the carcass, a first approximation of the meat layer thickness affected by drying is obtained from an analytical analysis as a semi-infinite solid. The model is solved numerically and it is validated with experimental data from the literature. Results of heat load and weight loss are compared to models proposed by other authors. Temperature and surface water activity evolution, and temperature and water content profiles are analyzed also. Finally, a sensitivity study is carried out on the main result of the model, total evaporated mass, varying heat convection coefficient and radiative cooling. It is found that there is a convective heat transfer coefficient that maximize the evaporative losses, so it is important to operate far from this point in order to reduce the evaporated mass. Furthermore, radiation during the meat cooling process turns out to be an interesting method to rapidly cool meat without increasing the evaporated mass (radiation cooling). Results shows that combining properly the convection and radiation heat transfer, evaporation losses can be reduced.

Keywords: Beef cooling, radiative heat transfer, convective heat transfer, mass transfer, evaporative weight loss.

*urquiola@fing.edu.uy

Nomenclature

a_w	product water activity
c_P	specific heat
$c_{P_{HA}}$	humid air specific heat
D_m	equivalent mass diffusivity of water in meat
Gr	equivalent Grashof number
Gr_m	mass Grashof number
Gr_t	thermal Grashof number
HR	air relative humidity
h_t	convective heat transfer coefficient
h_{t_F}	forced convective heat transfer coefficient
h_{t_N}	natural convective heat transfer coefficient
h_m	convective mass transfer coefficient
h_{m_F}	forced convective mass transfer coefficient
h_{m_N}	natural convective mass transfer coefficient
h_R	radiative coefficient
h_{fg}	water latent heat of evaporation
k	thermal conductivity
Le	Lewis number
M_a	air molar mass
M_{da}	dry air molar mass
m_{ds}	meat dry mass
m_T	total meat mass
m_w	meat water mass
Nu	Nusselt number
Pr	Prandlt number
$\dot{Q}''_C$	convective heat flux
$\dot{Q}''_E$	evaporative heat flux

Nomenclature

$\dot{Q}''_R$	radiative heat flux
Ra	Rayleigh number
Re	Reynolds number
R_w	ideal gas constant for water
Sc	Schmidt number
Sh	Sherwood number
T	temperature
t	time
x	distance
X_m	product surface water content, $\mathrm{kg}_{water}/\mathrm{kg}_{drysolid}$
β_m	coefficient of expansion due to concentration changes
ρ	mean density
ρ_{da}	dry air density
ρ_m	meat density
ρ_l	meat water content
ρ_v	air water vapor density
$\rho_{v,sat}$	water vapor density of saturated air
Subscripts	
a	air
i	initial
s	surface
w	wall

1. Introduction

In meat industrial process, during the first 24 hours postmortem a complex chain of energetic, biochemical and physical changes takes place, which result in the conversion of muscle to meat [1, 2]. The rate and extent of postmortem metabolism (mainly pH decline) significantly impact on meat quality attributes (color, texture and water-holding capacity). Muscle temperature during this period post slaughter affects metabolic reactions, and hence the meat quality development [2], so it is an important factor to be controlled during beef cooling.

Usually, this process occurs in a cooling chamber with forced air circulation and controlled air temperature and humidity. In this process, the carcasses hot and wet are cooled with air, by combining heat and mass transfer from the surface. As surface water evaporates, meat water diffuses from the interior to the surface, rewetting it. This phenomena entails a total beef carcass weight loss which is around 2% [3–6], which implies an economic loss for the industry [7]. Heat loss occurs by convection, radiation and water evaporation. From an initial analytical estimate, it is obtained that radiative heat transfer has an effect of the same order of magnitude as the convective one.

There are several works in the literature that deal with the numerical modeling of heat and mass transfer during beef carcass chilling. Mallikarjunan and Mittal [6] proposed a 2D model to determine the temperature profile evolution and weight loss. It was solved using finite elements in five zones with uniform cross-sections. Experimental data was collected and model results were in good agreement with them. Davey and Pham [8] developed a finite difference model to predict heat load and weight loss, approximating beef side geometry combining cylinders and slabs.The model was compared with experimental data and they conclude that despite having limited precision, reasonable results are obtained that allow for practical designs. Davey and Pham [9] proposed another model using 2D finite elements over 13 beef carcass sections. Results of heat load an weight loss where contrasted with their experimental data. This model results more accurate than the finite differences model developed earlier, with an added advantage that it can predict local temperatures. Trujillo and Pham [10] proposed a CFD model for a 3D beef side using the tree step method, calculating local heat and mass transfer convective coefficients. A separate 1-D grid was used to calculate the moisture diffusion in the meat. Heat load, temperature profiles, weight loss and water activity were calculated. Results were contrasted with Davey's experimental data and results from their models [8, 9, 11]. Temperature predictions agree with experimental data better than the other models, but weight loss was overpredicted. Pham et al. [12] presented a combined model where CFD was used for convective coefficients calculation, and 2D and 1D grids were used for heat and mass transfer in beef carcass, respectively. The model was verified by existing and new data on heat load, temperatures, weight loss and surface water activity. It was considered a reasonable alternative that reduced significantly the computational time compared to their previous work [10]. Kuffi et al. [4] developed a CFD model in a beef side 3D geometry, including postmortem reaction kinetics, to predict product quality during chilling, which was validated with their experimental measurements. The model predicted adequately the measured temperature profiles at different positions, and it allows to study the effect of relevant cooling parameters on the rate and uniformity of cooling and meat quality.

Modeling heat and mass transfer in a beef side, some difficulties arise that must be overcome by making simplifications and approximations, in order to best represent the real problem to be studied. Some of the most relevant difficulties are: uncertainty in the geometry, uncertainty in the thermophysical properties, uncertainty in heat and mass transfer convective coefficients (forced and natural), uncertainty in surface drying penetration and length scale differences between temperature and water content gradients, and the interdependence of heat and mass transfer, considering separately convection and radiation.

In the present work a 3D model of heat and mass transfer in a beef carcass during slaughter and cooling process is proposed, with the aim of predicting evaporative weight loss and the effect of convection and radiation heat transfer on it. Regarding the structure of the paper, section 2 describes the heat and mass transfer model, the main governing equations and its initial and boundary conditions, thermophysical properties, geometry adjustment, and meshes used. Besides, a rough estimation of surface layer affected by drying is done. Model validation with experimental data and other models from the bibliography is presented in section 3. Finally, in section 4, a sensitivity analysis of the evaporative weight loss is performed, independently varying the convective and radiative cooling mechanisms.

2. Model description

A model of heat and mass diffusion in a beef side, considered as a uniform porous solid, is represented. Uniform convective coefficients (heat and mass), calculated form correlations, are used over the entire surface as boundary conditions. Radiation heat transfer is considered, assuming a single beef side in a cooling chamber. Surface mass transfer is modeled considering forced and natural convection, taking into account the variations in water activity. Experimental measurements reported by Davey [11] are used as a reference (run 18) to validate the proposed model. Slaughter (2 hours) and cooling processes (20 hours) are modeled sequentially, assuming uniform initial properties. Thermophysical properties are calculated from data presented by Davey [11]. Mesh is adapted to have a large refinement near the surface in order to correctly model the mass diffusion, without excessively increasing computational time (see sections 2.5 and 2.6). An analytical estimation of surface layer affected by drying is proposed for mesh design, and validated with numerical results. A mesh-independence study is also presented.

2.1. Main governing equations

Heat transfer inside beef carcass is modeled using the transient heat equation for a solid (wet meat). Although in the beginning postmortem there are exothermal biochemical reactions (using the same procedure as Davey and Trujillo), the heat source term is not used. Instead it is assumed a bigger initial temperature, as if heat generation occurred all at the initial time [10, 11]. In order to simplify the model, the effects of crust formation and surface fat layer as a water transfer barrier are not considered in the present work. Therefore, equation 1

$$\rho c_P \frac{\partial T}{\partial t} - \nabla \cdot (k \nabla T) = 0 \tag{1}$$

is used, where ρ, c_P and k are mean density, mean specific heat and mean thermal conductivity of the solid respectively.

There are several works where meat evaporative losses during cooling process are evaluated, but many of them do not model mass diffusion in meat, assuming a constant and uniform surface water activity [4, 8, 9]. However, water activity may vary significantly during cooling process and over all carcass surface (see Trujillo and Pham [10]). Since water activity depends on meat water content, it is essential to model water content inside the beef carcass, to take its variations on the surface into account.

Therefore, in this work it is considered that water moves by mass diffusion inside beef carcass and it is modeled using equation 2,

$$\frac{\partial \rho_l}{\partial t} - \nabla \cdot (D_m \nabla \rho_l) = 0 \tag{2}$$

where ρ_l is meat water content in kg/m^3 and D_m is the equivalent mass diffusivity (that represents all water movement effects inside beef carcass) [13]. In order to calculate D_m, the correlation obtained by Trujiilo et al. [13] is used and presented in Table 5.

2.2. Boundary conditions

The air conditions around the beef vary throughout the different stages, but are assumed to be constant at each one of them. In this case, two stages are continuously modeled: slaughter process lasting 2 hours and cooling process lasting 20 hours. Temperature and relative humidity values imposed to our model are averaged values experimentally found by Davey [11]. In slaughter process air conditions are 25°C and 63% relative humidity, and during cooling process they are 4.88°C and 98%.

Heat loss from meat surface is due to convection, radiation and water evaporation, so boundary condition can be written using the Fourier's Law as in equation 3.

$$-k\frac{\partial T}{\partial x} = \dot{Q}''_C + \dot{Q}''_R + \dot{Q}''_E \tag{3}$$

Heat flux transferred by convection ($\dot{Q}''_C$) is calculated from equation 4,

$$\dot{Q}''_C = h_t(T_s - T_a) \tag{4}$$

where T_s is the beef side surface temperature, T_a is the surrounding air temperature and h_t is the convective heat transfer coefficient. Convective coefficients could be obtained from experimental measurements [14], empirical correlations for simple geometries [6, 8, 9, 11], or by CFD [4, 10, 12]. In the present work are studied scenarios with different convection coefficients and taking into account the excessive computational time of doing CFD, it is decided to set a single convection coefficient over entire surface of beef side. It is calculated from the empirical correlation presented in equation 5 [11, 15],

$$h_t = (h_{t_F}^3 + h_{t_N}^3)^{1/3} \tag{5}$$

which combines forced and natural convective coefficients, h_F and h_N, in a single one. Coefficients are calculated assuming beef side as a vertical plate of length $L = 2.35$ m (for run 18) with parallel flow, as used Davey [11]. Forced convective coefficient is calculated from the correlation present in equation 6 [16],

$$Nu = 0.664 Re^{0.5} Pr^{0.33} \tag{6}$$

taking the air velocity $v = 0.598$ m/s measured by Davey [11] for run 18, and air properties at mean temperature for each process. Values obtained are presented in table 1. In natural convection, momentum equation is coupled to heat and mass transfer equations, since buoyancy term depends on temperature and species concentration gradients. Thus, both phenomena influence airflow. However, if $Pr \approx Sc$ ($Le \approx 1$), as temperature and species concentration field turn out to be analogous, Grashof number can be estimated as $Gr_t + Gr_m$ [16, 17], where Gr_t is the usual Grashof number for heat transfer (equation 7)

$$Gr_t = \frac{L^3 g}{\nu^2} \beta_t (T_w - T_a) \tag{7}$$

and Gr_m is the mass Grashof (equation 8),

$$Gr_m = \frac{L^3 g}{\nu^2} \beta_m (\rho_{v_w} - \rho_{v_a}) \tag{8}$$

with

$$\beta_t = -\frac{1}{\rho} \left(\frac{\partial \rho}{\partial T} \right)_{\rho_v, P}$$

and

$$\beta_m = -\frac{1}{\rho} \left(\frac{\partial \rho}{\partial \rho_v} \right)_{T, P}$$

Additionally, Nusselt correlations can be used to calculate Sherwood number, changing Pr by Sc and considering $Gr = Gr_t + Gr_m$ to calculate Ra. In case of water vapor in air, as in the present work, the assumption $Le \approx 1$ is acceptable. In the conditions of this work, Gr_m is around 25% of Gr_t, indicating that the water vapor concentration gradients in the air have a non-negligible effect on the air flow. Natural convective coefficient is calculated from Nusselt correlation in equation 9 [17],

$$Nu = \left(0.825 + \frac{0.387 Ra^{1/6}}{\left[1 + (\frac{0.492}{Pr})^{9/16}\right]^{8/27}}\right)^2 \quad (9)$$

valid for Rayleigh number bigger than 10^9, by using air properties at a mean temperature for each process. Coefficients obtained are presented in table 1. As can be seen, forced and natural coefficients are of the same order of magnitude, but the natural one is a bit bigger. The equivalent coefficient calculated with equation 5 results something greater than the natural one, and the order of magnitude is the same as the ones found in the literature [10, 11, 14] for similar air flow velocities, which vary between 0 and 10 W/m^{2}K.

Table 1: Convective heat transfer coefficients (W/m^{2}K)

	Slaughter	Cooling
Forced convection	1.97	1.97
Natural convection	3.08	3.16
Equivalent coefficient	3.33	3.40

Heat flux transferred by radiation ($\dot{Q}''_R$) is modeled assuming that a single beef side is inside a large cold chamber, so for the purposes of radiative exchange the room can be assumed as a black body. Under this hypothesis, establishing a uniform temperature, T_w, on chamber walls, floor and ceiling (considered as a unique temperature), radiation heat transfer is calculated with equation 10,

$$\dot{Q}''_R = \sigma \varepsilon (T_s^4 - T_w^4) \quad (10)$$

where ε is meat emissivity and its value is assumed to be 0.9 [15, 16]. In equation 10, $T_s^4 - T_w^4$ can be rewritten as $(T_s^2 + T_w^2)(T_s + T_w)(T_s - T_w)$, where temperatures are absolute. Keeping walls temperature fixed, the variation in meat surface temperature throughout the cooling process makes the term $T_s - T_w$ vary significantly, while the term $(T_s^2 + T_w^2)(T_s + T_w)$ varies slightly. It is usual to combine convection and radiation heat transfer in an effective heat transfer coefficient, assuming that the temperature of the walls is equal to that of the air ($T_w = T_a$) [15]. The term $\sigma\varepsilon(T_s^2 + T_w^2)(T_s + T_w)$ is h_R in equation 11.

$$\dot{Q}''_C + \dot{Q}''_R = (h_t + h_R)(T_s - T_a) \tag{11}$$

The combination of these coefficients in a single one must be considered carefully since radiative coefficient (h_R) is not related to the mass convective coefficient by Lewis analogy. In the proposed model, radiative coefficient variation (due to T_s variation) is considered during slaughter and cooling processes, since its value is of the same order of magnitude as the convective one (for T_s=15°C, h_R=4.6 W/m^{2}K).

The evaporative heat loss ($\dot{Q}''_E$) is the energy required to evaporate water from the product surface. This heat loss is calculated as the evaporated mass multiplied by phase change latent energy h_{fg}, as in equation 12,

$$\dot{Q}''_E = \dot{m}''_{evap} h_{fg} = h_m(\rho_{v,s} - \rho_{v,a})h_{fg} \tag{12}$$

where h_m is the convective mass transfer coefficient, and $\rho_{v,s}$ and $\rho_{v,a}$ are water vapor densities on meat surface and on air, respectively. The convective mass transfer coefficient combines forced and natural phenomenons and it is calculated using an equation analogous to equation 5, $h_m = (h_{m_F}^3 + h_{m_N}^3)^{1/3}$. Forced convective mass transfer coefficient is obtained from Lewis analogy expressed by the equation 13,

$$h_{m_F} = \frac{h_F}{\rho_{da} c_{P_{HA}}} Le^{1-n} \tag{13}$$

which is valid in forced convection conditions. $c_{P_{HA}}$ is the humid air specific heat and ρ_{as} is the dry air density. The values obtained are presented in table 2. The natural mass convective coefficient is calculated using the the Grashof number calculated as $Gr_c + Gr_m$, and Sherwood is calculated using the Nusselt

Table 2: Convective mass transfer coefficients (m/s)

	Slaughter	Cooling
Forced convection	1.84×10^{-3}	1.76×10^{-3}
Natural convection	2.85×10^{-3}	2.78×10^{-3}
Equivalent coefficient	3.09×10^{-3}	2.99×10^{-3}

correlation (equation 9) substituting Pr by Sc. The equivalent mass transfer coefficients are practically the natural ones, as it is shown in table 2.

Finally, equation 3 can be rewritten as equation 14.

$$-k\frac{\partial T}{\partial x}\bigg|_s = (h_t + h_R)(T_s - T_a) + h_m(\rho_{v,s} - \rho_{v,a})h_{fg} \tag{14}$$

The boundary condition for the mass transfer equation (2) is given by Fick's Law and it is equal to the mass of water transferred by convection at the surface (equation 15).

$$-D_m\frac{\partial \rho_l}{\partial x}\bigg|_s = h_m(\rho_{v,s} - \rho_{v,a}) \tag{15}$$

The vapor density on the surface and in the air are calculated from equations 16 y 17,

$$\rho_{v,s} = \frac{M_{da}}{M_a}\frac{a_w\left(\frac{p_{v,sat}}{p_T}\right)}{1 - a_w\left(\frac{p_{v,sat}}{p_T}\right)}\rho_{da} \tag{16}$$

$$\rho_{v,a} = \frac{M_{da}}{M_a}\frac{HR\left(\frac{p_{v,sat}}{p_T}\right)}{1 - HR\left(\frac{p_{v,sat}}{p_T}\right)}\rho_{da} \tag{17}$$

which depend on the water activity a_w and air relative humidity HR, respectively. Meat water activity varies from one point to another over the beef side and throughout the cooling process [10]. Although a_w varies between 0.95 and 1, it is important to take into account these variations to avoid incorrect estimation of heat losses due to evaporation [15]. Trujillo et al. [18] measured experimentally moisture sorption isotherms of beef in the range 5 to 40°C, and they compared with GAB and Lewicki correlations. GAB correlates adequately for a_w less than 0.9 and Lewicky for values between 0.9 and 1 [18]. In order to obtain a single and adequate correlation in the range of 0.6 to 1, the experimental values measured by Trujillo et al. [18] were adjusted obtaining a curve of X_m as a function of a_w, where X_m is the meat water content in the surface in $\text{kg}_{water}/\text{kg}_{dry\,solid}$. In the model it is necessary to introduce a_w as a function of ρ_l, so the relation between Xm and ρ_l is needed. This is presented in equation 18,

$$\rho_l = \frac{m_w}{m_T}\rho_m = X_m \frac{m_{ds}}{m_T}\rho_m \tag{18}$$

considering total mass, water mass and dry solid mass, calculated from beef side composition defined by Davey [11]. Combining the experimental data [18] and equation 18, the correlation proposed for water activity is presented in equation 19 with a correlation coefficient of R=0.9955.

$$a_w = e^{0,2619-45,56/\rho_l-0,0328ln(\rho_l)} \tag{19}$$

2.3. Initial conditions

The problem is modeled form the beginning of the slaughter process, assuming a uniform initial temperature in the whole beef side, taking into account the temperature increase because of the rigor mortis process. The initial temperature value is taken from the Davey's work [11] for run 18, and it is 42,4°C. After that, cooling process begins with the temperature field obtained at the end of slaughter process. For mass diffusion equation, the initial condition is a water content of 75% in weight on wet basis, taken form Trujillo el al. [10]. It means an initial water content of 834 kg/m^3.

2.4. Thermophysical properties

The beef carcass thermal properties are calculated from the values presented by Davey [11], from the beef side constitution corresponding to run 18. In order to simplify the model, it is assumed uniform average properties in whole beef side, taking into account the muscle, fat and bone phases. The beef side corresponding to run 18 weighed 108 kg and the mean fat thickness was 6 mm. From these values and using the correlations established by Davey [11], the weight % of each phase are calculated as is shown in table 3. In turn, muscle (lean meat) and beef fat composition presented in the table 4 were determined.

Table 3: Beef carcass constitution.

Phase	% weight
Muscle	59.42
Fat	15.75
Bone	24.83

Table 4: Phases composition.

Component	Lean meat (%)	Beef fat (%)
Water	75.9	10.4
Protein	19.8	3.5
Fat	3.2	85.1
Ash	1	1

Table 5: Thermophysical properties

Property	Value
c_p	3585 kJ/kgK
k	0.391 W/mK
ρ	1112 kg/m^3
D_m $[\mathrm{m}^2/\mathrm{s}]$	$4.67 \times 10^{-5} \exp(-3757.26/T)$

Form the beef side constitution and phases composition data, mean density and specific heat are calculated, obtaining the values presented in table 5. In order to estimate the equivalent thermal conductivity it is used a parallel model that combines thermal conductivities of lean meat, fat and bone. The conductivities of lean meat and fat could be calculated from different models presented by Hoang et al. [19], as Levy model and Dul'Nev and Novikov model which have very good results for lean beef. In the present work Levy model [20] is used since it is the one used by Davey [11]. Lean meat is assumed composed by a continuous water phase and the other components scattered. The same is assume for fat, considering the fat as the continuous phase. The vale used for bone conductivity is 0,26 W/mK [21]. In table 5 the equivalent thermal conductivity is also presented. The values obtained for specific heat, density and thermal conductivity are very similar to those used by Trujillo et al. [10] ($c_P = 3407$ kJ/kgK, $\rho = 1111$ kg/m^3, $k = 0.397$ W/m^{2}K).

2.5. Geometry

A geometry from an image library, obtained from a 3D scan of a real beef side, is used. This is modified in order to obtain the same total mass as reported by Davey [11], which is 108 kg for run 18, and the same area/volume ratio. This last parameter is expected to significantly affect the results, and this was later confirmed during the simulations. Therefore, the original geometry is modified in a non-isotropic way to obtain an area/volume ratio of 24.9 1/m. This value was calculated from the estimation of the area and volume of the carcass obtained from the geometric measurements reported by Davey [11] for 14 sections. The geometry is adjusted using COMSOL's scale tool considering different coefficients in each direction, always maintaining the total mass and therefore the total volume (using the previously calculated mean density), besides the beef side total length reported by Davey [11], 2.35 m.

2.6. Numerical resolution

The model is implemented on COMSOL Multiphysics ® software using a backward differentiation formula implicit method. The time step is automatically calculated by the software. Outputs, temperatures and water content were shown every 360 s.

As water diffusion through meat is relevant only in a thin layer near the surface [10, 12, 22], in the present model two meshes are combined as it was done by Trujillo et al.[10], who defines a surface layer 24 mm thickness as the interest zone for mass diffusion in a beef side which was meshed separately, assuming an unidirectional mass diffusion. In the present model an automatic physics-controlled tetrahedral mesh is used for the interior domain, and a boundary layer mesh is used for the surface layer. This combination (see figure 1) allows to work with a greater refinement near the surface, maintaining a coarse mesh, suitable for modeling heat diffusion, in the rest of the domain. The tetrahedral mesh has 502,380 domain elements and 13,480 border elements. For the boundary layer, 32 layers of different thickness were defined, starting at 0.2 mm on the surface and increasing by 7 % each one with respect to the previous one, since the water content gradients are greater the closer to surface. The boundary layer mesh thickness is defined as 22 mm, similar to the one used by Trujillo et.al [10].

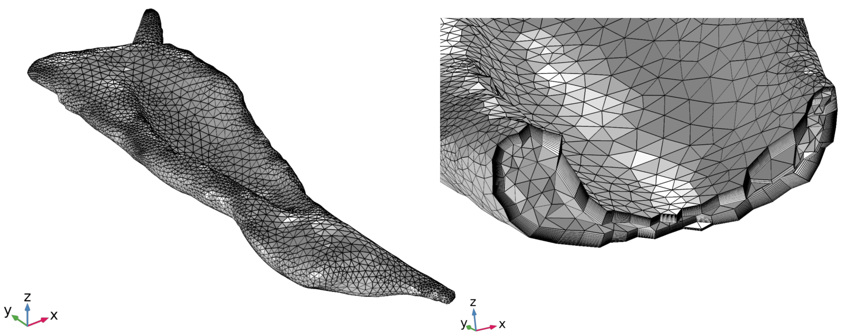

Figure 1: Meshes used in the model: tetrahedral mesh and boundary layer mesh.

Different refinements were tested in order to verify the mesh independence for tetrahedral mesh, keeping the boundary layer mesh unchanged. Each of these meshes has the number of elements presented in table 6. Using the finer one as a reference (mesh 5), the error in results of heat load and cumulative evaporated mass were calculated for each time during 20 hours of chilling process. The heat load $\dot{Q}$ is the total heat lost by the beef side surface, that is the sum of sensible and latent heat transferred, calculated from equation 20,

$$\begin{aligned}\dot{Q}(W) &= (h_t + h_R)(T_s - T_a) + \\ &hm\left(\frac{aw\frac{p_{v,sat}}{p_T}}{1 - aw\frac{p_{v,sat}}{p_T}}\rho_{as} - \frac{HR\frac{p_{v,sat}}{p_T}}{1 - HR\frac{p_{v,sat}}{p_T}}\rho_{as}\right)h_{fg}\end{aligned} \tag{20}$$

which is obtained by combining equations 14, 16 and 17. Cumulative evaporated mass is calculated by integrating equation 21 over beef surface and over time.

$$\dot{m}'' = h_m(\rho_{v,s} - \rho_{v,a}) = \\ \frac{h_m}{R_w}\left(\frac{p_{v,sat}(T_s)a_w}{T_s} - \frac{p_{v,sat}(T_a)HR}{T_a}\right) \tag{21}$$

Table 6 shows the maximum relative error obtained for each refinement. As can be seen, the maximum error decreases as the refinement increases. Finally, mesh 4 is used for the model, which has maximum errors of 0.876% in heat load and 0.172% in weight loss, which are considered acceptable for this work, with a low computational cost.

Table 6: Mesh independence.

	Mesh 1	Mesh 2	Mesh 3	Mesh 4	Mesh 5
Elements Domain/Boundary	92047/2678	154662/4416	242416/6770	502380/13478	678187/17002
Max. heat load error (%)	5.569	5.014	2.574	0.876	-
Max. weight loss error (%)	0.879	1.028	0.518	0.172	-

In relation to boundary layer mesh independence, five different refinements were tested, always keeping a thickness of 22 mm. To compare the different meshes, water density profiles inside the meat were observed and the chosen mesh is the one that results in a smoothed profile, without excessively increasing the calculation time.

2.7. Analytical analysis of drying thickness

In the present work, with the aim to obtain an estimate of the interest thickness under our conditions, and assuming that it is very small respect to beef side dimensions, the semi-infinite solid model is used. Based on the analytical solutions for heat transfer in a semi-infinite solid, an analogous solution could be used for mass transfer, since equations 1 and 2 are analogous. After evaluating different analytic solutions, corresponding to different imposed boundary conditions, it was concluded that the case of fixed surface concentration (or surface water density in this case) and imposing this value equal to zero, results in an adequate estimation for the maximum possible affected width. A more detailed analysis can be found in Appendix A. The affected layer width is therefore calculated with the following simple equation 22,

$$\delta_{99} = 3.66 D_m t \tag{22}$$

which corresponds to the length within the medium at which the water density is 99% of the initial condition. The layer thickness obtained is 18 mm, which is of the same order of magnitude than the one used by Trujillo and Pham [10] (24 mm). Due to the simplicity of this equation, it should be useful for determining the mesh layer to be densified for mass transfer calculations, but also as an estimation of the maximum possible drying penetration depth without the need to perform numerical calculations.

3. Model validation

In this section is validated the proposed model using the experimental data collected by Davey [11], comparing the obtained results of heat load and evaporative weight loss throughout the cooling process. Temperature evolution at four points of the beef side are compared, seeking to identify the measurement points taken by Davey. Additionally, a comparison is made with the results obtained with other models made by Davey [8, 9, 11] and Trujillo [10].

3.1. Heat load

The heat load is calculated throughout whole process, slaughter and cooling, although the reference literature presents only experimental measurements during the cooling process. In figure 2a, the values obtained for each instant are compared with those collected experimentally by Davey [11] and the ones predicted by Davey et al. [8, 9] with finite differences (FD) and finite elements (FE) models, and by Trujillo et al. [10] with a CFD model. In figure 2b heat load relative percentage errors of different models to experimental values are plotted. From 10 hours, the relative errors become very large as the heat load becomes very small. As can be seen, the present model correctly predicts heat load loses by the beef side during entire cooling process with a good fit to experimental data, even better than the other models from 14 hours onwards.

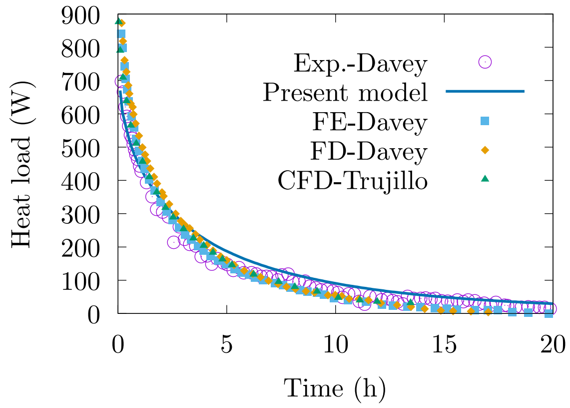

(a)

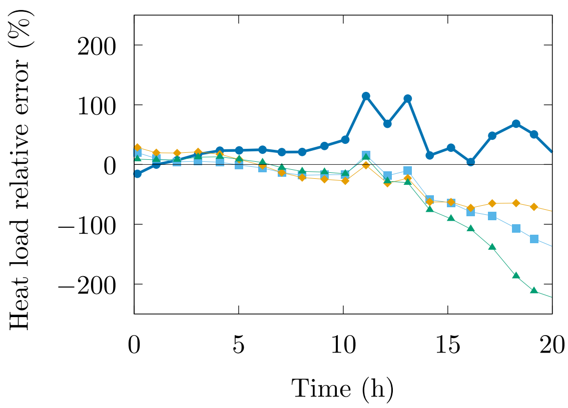

(b)

Figure 2: (a) Heat load losses by the surface during the cooling process. Comparison of the proposed model results with experimental data and other models. (b) Heat load relative error respect to experimental values.

3.2. Evaporative weight loss

Beef side evaporative weight loss is one of the most important results of this model, since it is a mayor interest to reduce it. Figure 3a presents cumulative weight loss during cooling process obtained with the proposed model, which is compared to experimental data collected by Davey [11] and results of models proposed by Davey et al. [8, 9], and Trujillo et al. [10]. Figure 3b shows the relative percentage error from different models respect to experimental values. Proposed model presents a good concordance with experimental results, reaching after 20 hours a total evaporated mass of 1.35 kg (which represents a 1.28%

of total beef side weight) with an error of 2.9 %, which is smaller to errors obtained with the other models (see table 7). Besides, the other models underpredict the total evaporated mass while the presented model slightly overpredict it. As the convective mass transfer coefficients for each process are calculated with thermal properties at a mean temperature, it is smaller than the real one in the first hours and bigger at the end of the process. This could explain why during the first hours evaporation rate predicted (slope in figure 3a) is smaller than the experimental one, and during the last hours it is a little bigger. However, at the end of the process the proposed model presents a growth rate of cumulative weight loss more similar to the experimental one than the other models.

The weight loss results of the different models were compared to experimental data using root mean square error (RMS) along the chilling process. The results, presented in table 7, show that the best model is that of Trujillo et al. [10] which uses CFD to calculate local convective coefficients. The RMS for the present model, despite its simplifications, is of the same order and it is lower than those of finite difference and finite elements models from Davey et al. [8, 9].

Table 7: RMS error and final relative error (after 20 hs) in weight loss, comparing against the experimental data from Davey ??.

Model	RMS Error (kg)	Final weight loss relative error (%)
Present model	0.056	2.9
FD-Davey	0.618	
FE-Davey	0.109	14.8
CFD-Trujillo	0.040	6.5

4. Results and discussion

In this section, the results of temperature evolution during cooling, temperature profiles, meat water content, and water activity are qualitatively analyzed and compared with other models. It is important to acknowledge that the proposed model has some limitations that could be improved, despite achieving good results. Although a geometry derived from a 3D scan was used and scaled to match the volume and surface area of the reference case (trial 18 of Davey

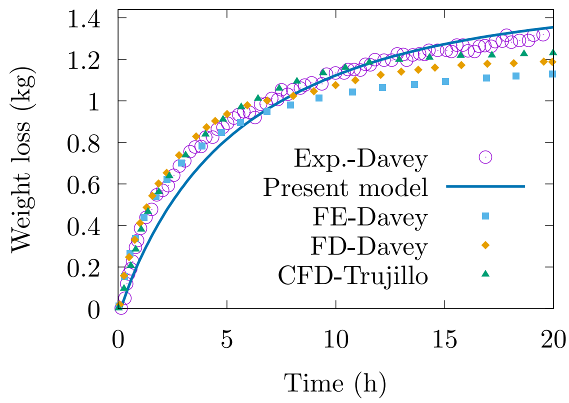

(a)

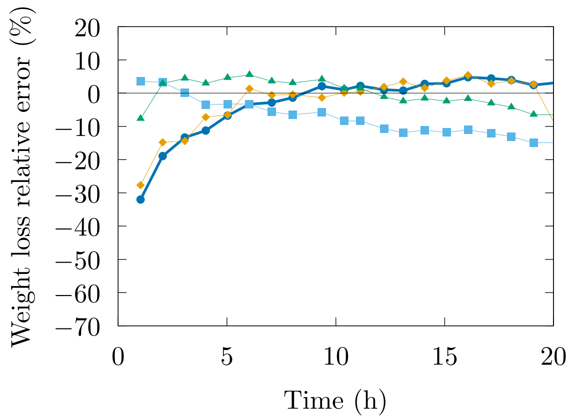

(b)

Figure 3: (a) Cumulative weight loss during the cooling processes. Comparison of the proposed model results with experimental data and other models. (b) Weight loss relative error respect to experimental values.

et al.), the actual geometry remains unknown, posing a source of uncertainty in the model. The distribution of meat, fat, and bones in a beef carcass varies from one animal to another, presenting a complex determination. Even if this distribution were known, incorporating it into the model would involve considering regions with different thermophysical properties and their interaction, thereby increasing its complexity. Therefore, assuming uniform properties for the meat side is a simplification that also introduces uncertainty into the model. Related to this, as mentioned in Section 2.4, there are different models to estimate thermal conductivity based on composition [19]. In this work, the Levy model was used, but there might be other models that better fit the experimental measurements. Finally, heat and mass transfer convective coefficients varies over the beef side surface and during the processes. Local heat transfer coefficients could be calculated by CFD, which implies a more complex model and a higher computational cost. Despite all these simplifications, the model is considered to be validated. The impact of convective coefficient values and the radiative cooling in weight loss are analyzed in this section by a sensitivity analysis.

4.1. Results of temperature and meat water content

With the aim of analyzing the results and to compare some of them with those obtained by Davey [8, 9, 11] and Trujillo et al. [10], two cross-sections of the beef side are defined, one in the area of the hind leg and other in the loin. These sections are used to analyze the evolution of temperature and moisture content throughout the cooling process. Furthermore, in each section a cut line in the x direction and two reference points (in the surface and in the center) are arbitrarily defined, in order to coincide the boundary and interior temperature with the reference ones. In figure 4a hind leg section is shown, indicating the location of cut line and reference points.

4.1.1. Temperature

In order to make a qualitative comparison of temperature evolution during the cooling process, between the proposed model and the results obtained by Davey [8, 9, 11] and Trujillo et al. [10], the points indicated in Figure 4a are defined for leg section. Davey experimental measurement points are used as a reference [11] to locate the surface and center points in each section. However, information about the specific location of sensor is not available in Davey's work, so the points in this work are arbitrarily chosen to have approximately the same cooling initial temperature to the experimental values. Figures 4a shows the initial cooling process temperature distribution in the hind leg section.

In figure 4b temperature profiles are shown along hind leg cut line, every 2 hours, from the beginning of slaughter process. Initially the meat is assumed to be at a uniform temperature. After 2 hours, when cooling process begins, surface temperature reached almost 25 °C, while the center practically is not cold. At this time the greatest surface heat loss is obtained (maximum slope of the

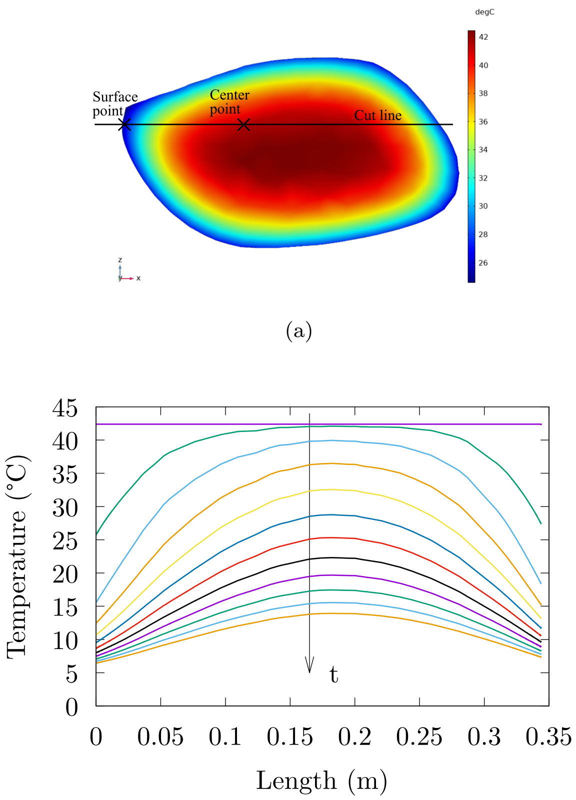

(a)

(b)

Figure 4: (a) Hind leg section, location of cut line and reference points. Temperature color map at time 2 hours (beginning of cooling process). (b) Temperature profile evolution during slaughter and cooling processes (every 2 hours) along the hind leg cut line.

temperature profile in the surface), since the ambient air temperature suddenly changes from 25 °C to 5 °C. From this moment on, heat loss in the surface progressively decreases (slope of the surface temperature profile decreases), slowing down the cooling rate more and more. Temperature gradient inside the meat decreases, lowering the core temperature. Finally, at 22 hours a more uniform profile is reached with a maximum temperature difference of 7.5 °C between the center and the surface.

Figures 5 and 6 show the temperature evolution curves in the surface and center points of leg and loin sections respectively, during the cooling process. In order to evaluate the results obtained with the proposed model, Davey's experimental values [11] and those obtained with Davey's EF and DF models [8,

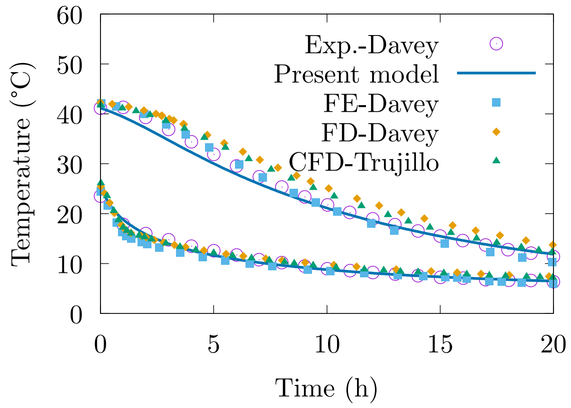

Figure 5: Temperature evolution in surface (down) and center (top) points in hind leg section during cooling process. Comparison of the proposed model with the experimental values and other models.

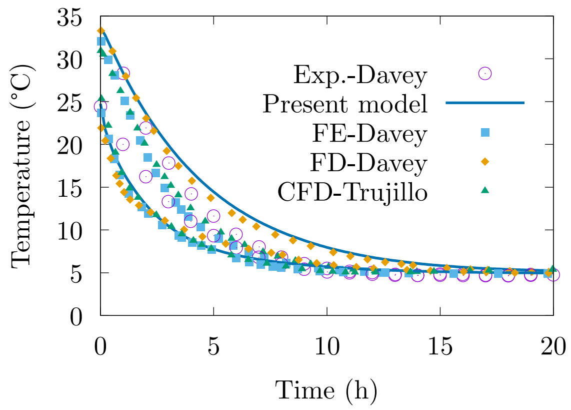

Figure 6: Temperature evolution in surface (down) and center (top) points in loin section during cooling process. Comparison of the proposed model with the experimental values and other models.

9] and Trujillo's CFD [10] are also plotted. It is observed that the temperautre evolution obtained with the proposed model are in concordance with the other models. To obtain a better fit, the exact location of the sensors on beef side and geometry should be known.

4.1.2. Meat water content

Water content inside the meat is evaluated from meat water density. As mentioned above, this density shows relevant variations only in a thin surface layer of around 18 mm. For this reason a boundary layer type mesh is used to obtain a greater refinement in this area. This profile penetrates throughout the process, reaching the greatest thickness at the end of the cooling process. In figure 7 the water density profile at the end of cooling process and the mesh used, in leg section, are shown superimposed in order to visualize the advance of density profile in relation to the boundary layer.

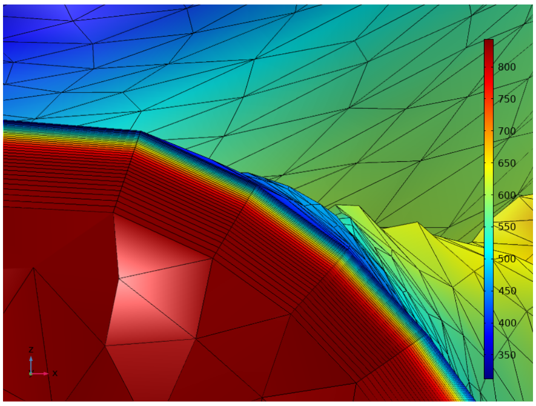

Figure 7: Meat water content distribution in leg section at the end of cooling process (22 hours), overlaid with the boundary layer mesh.

Figure 8 shows the water density profile in the meat, on the leg cut line defined above, in a thin layer near the surface, every two hours. In the initial 4 hours (2 hours of slaughter and 2 hours of cooling) the surface dries very quickly, since the evaporation rate is greater than the internal water diffusion rate. The water content on the surface decreases from 834 kg/m^3 to approximately 470 kg/m^3 in these 4 hours. After 6 hours, internal diffusion becomes more relevant, causing the surface to re-wet and surface water density progressively increase during the remaining 16 hours. Simultaneously, it is observed that the water density profile penetrates, increasing the thickness of the dried surface layer, reaching approximately 11 mm at the end of beef cooling (22 hours). This value is of the same order of magnitude, but smaller than the analytical estimation made in Section 2.7 (18 mm), as it was expected.

These results show that the surface does not dry completely during cooling, so it would seem reasonable not to consider the formation of crust acting as a barrier to water evaporation in the model.

Meat water activity affects the evaporation rate (equation 16) and it depends

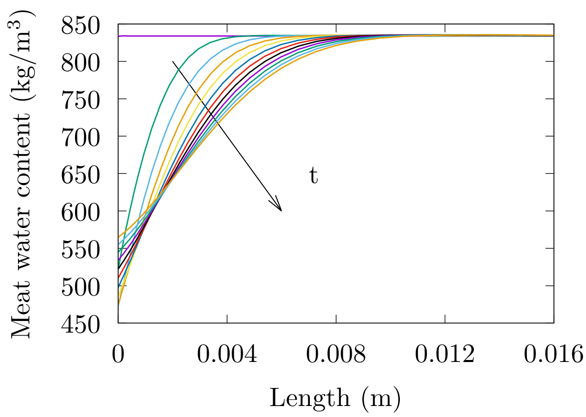

Figure 8: Meat water content profile evolution during slaughter and cooling processes (every 2 hours) along the leg cut line, in a thin layer near the surface.

on surface water content. Figure 9 shows the evolution of average water activity on the beef side and in the reference points, on the leg and loin surface, during the slaughter and cooling processes. Besides, water activity over whole surface is presented in a color map after 4 hours. Water activity varies between 0.96 and 0.99 as it was expected [15]. The water activity evolution is similar to the results of Trujillo and Pham [10], during the first hours water evaporation rate is higher than rewetting rate so the surface water activity decrease, reaching an average value of 0.96. Later, mass transfer potential decrease and the rewetting rate becomes bigger than evaporation rate, so water activity increase again but more slowly. Comparing reference points (leg and loin), it can be seen that water activity values are bigger in the leg than in the loin, as it is observed by Trujillo and Pham [10]. This is because the thinner parts in the beef side cools more quickly and therefore mass transfer potential decreases, reducing evaporated mass. This can be seen in the beef side color map, where the thickest parts have the lowest water activity values and the thinner parts have the higher ones.

Figure 10 shows evolution of real mass transfer potential considering water activity variation (equations 15 to 17) and the potential assuming a constant water activity $a_w = 1$, during the 22 hours. The real mass transfer potential is smaller than the other as expected, but it can be seen that the effect of water activity in the mass transfer potential is slight since the water activity values

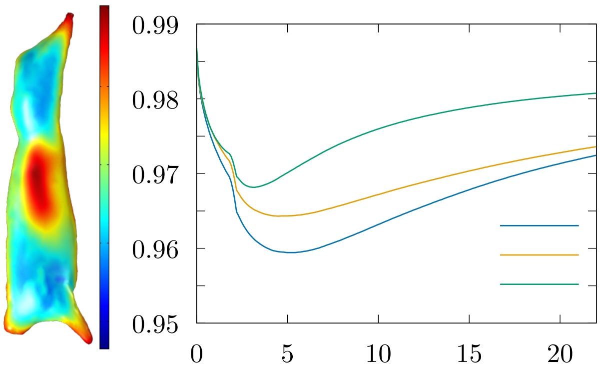

Figure 9: Beef side water activity for time 4 hours (left). Water activity evolution in time during the slaughter and cooling processes (right).

are relatively high.

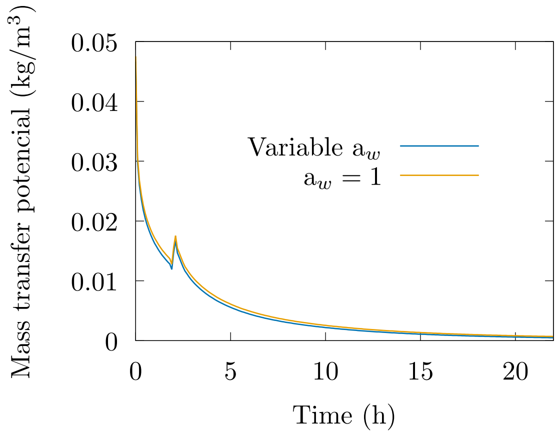

Figure 10: Mass transfer potential evolution during the slaughter and cooling processes.

If figures 8, 9 and 10 are analyzed together, it is seen that during the initial hours there is a high surface temperature and a high a_w, which implies a great potential mass transfer. During the initial 6 hours, as the surface temperature decreases, the same happens to a_w, both generating a decrease in potential (see figure 10). After that, the surface temperature continues decreasing, but now the a_w begins to increase. In this scenario, both factors have opposite effects on the potential. However, the temperature drop has a greater impact than the increase in the a_w on the potential, causing it to continue decreasing.

analysis Convective coefficients and the temperature of cold room walls affects the beef carcass weight loss. A sensitivity analysis is done in order to evaluate its impact in weight loss and the need to calculate them with greater precision. As a consequence, this analysis is a first step to explore alternatives for the cooling process in order to reduce the weight loss, which should be studied in depth in the future taking into account technological limitations.

4.1.3. Sensitivity analysis to convective coefficient values

In order to evaluate the impact of convective heat transfer coefficients on the main results of the proposed model, the evaporated mass, a sensitivity study is carried out by varying the convective coefficient during the cooling process from $0.5\,h_t$ to $10\,h_t$ (where h_t=3.4 W/m^{2}K and the range of variation is 1.7 to 34 W/m^{2}K). Values of convective coefficient during slaughter process is not changed, so the initial condition of cooling process is the same for any case. In figure 11 the cumulative weight loss during the cooling process is presented for different convective coefficients. Evaporative weight loss depends on two factors, the mass convective coefficient, which is directly proportional to the heat convective coefficient (assuming $Pr \approx Sc$ for natural convection) and the mass transfer potential which is directly related to meat surface temperature. The reference curve (violet) is obtained with the convective coefficient value of 3.4 W/m^{2}K. If the coefficient is reduced respect to the reference one, the evaporation rate drops significantly during the initial hours of the process. However, this decrease in evaporation makes surface cooling less, so that at the end of the process the potential for mass transfer increases due to a greater difference in temperatures between the meat surface and the air, increasing the evaporation rate. The total weight loss after 20 hours is reduced with respect to the reference one. When the coefficient is somewhat higher than the reference one, the evaporation rate increases during the initial hours. Nevertheless, as the surface cools faster, the potential for mass transfer decreases in the last few hours, decreasing the rate of evaporation. In any case, the overall effect after 20 hours is that the total evaporated mass increases. As the convective coefficient is further increased, the evaporation rate increases dramatically in the initial hours, and the surface cools very quickly, which means that the overall effect is to reduce the total evaporated mass. This means that there are values of the convective coefficient that maximize evaporative losses. This maximum can be seen in figure 12 in the curve for T_w=4.88°C.

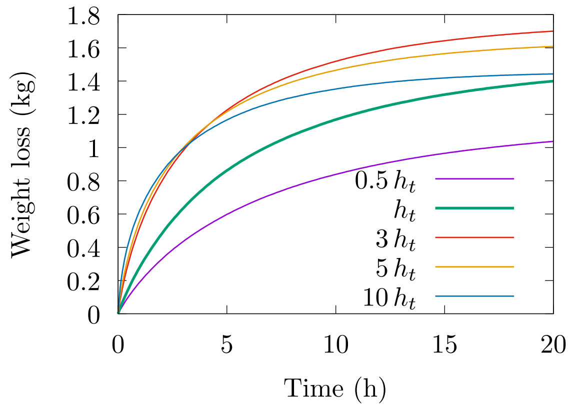

Figure 11: Cumulative weight loss during cooling process for different values of convective heat transfer coefficient.

4.1.4. Sensitivity analysis to radiative cooling

In the previous analysis, radiative heat lost in the surface is calculated keeping walls temperature equal to the air one $T_w = T_a$=4.88°C. The impact of radiative cooling variation is qualitatively analyzed, assuming that heat convective coefficient remains unchanged (h_t=3.4 W/m^{2}K). In Figure 13 cumulative weight loss for different arbitrary wall temperature values is presented. As can be seen, as walls temperature is reduced, total evaporated mass decreases significantly. This is because the meat surface temperature is reduced, decreasing mass transfer potential while mass convective coefficient remains constant. Unlike convective cooling, radiative cooling allows to decrees meat temperature without increasing evaporated mass, since mass transfer coefficient is not affected. This is an interesting way to be analyzed with the aim of reducing weight loss during beef carcass cooling process, that must be studied more carefully and rigorously.

Figure 12 also shows the effect of convective coefficient variation for different scenarios of radiative looses, changing the walls temperature arbitrarily. As the walls temperature decreases, total weight losses is less affected by changes in convective coefficient. It could be explain because when the walls temperature is reduced, radiative cooling becomes more relevant than the convective one, and therefore meat surface cooling is dominated by radiation. This means that mass transfer potential become more relevant than mass convective coefficient in mass transfer equation (21).

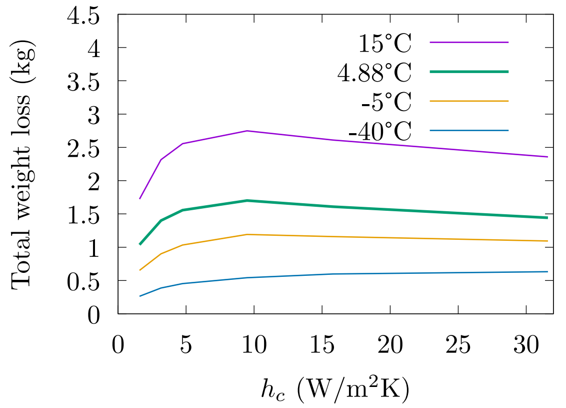

Figure 12: Total weight loss after 20 hours of beef cooling vs convective coefficients. Curves for different radiative heat transfer, varying the wall temperature T_w.

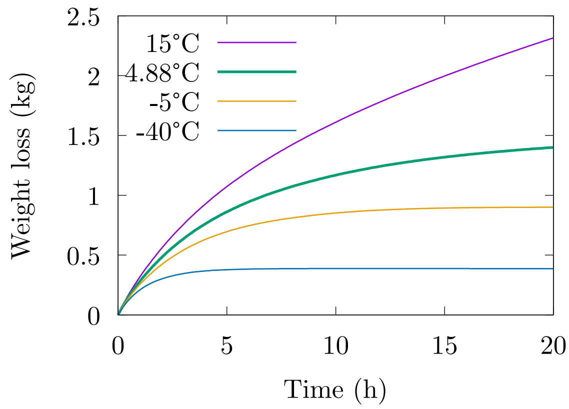

Figure 13: Cumulative weight loss during cooling process in different scenarios of radiative cooling (varying the wall temperature T_w), based on reference convective coefficients values.

5. Conclusion

Heat and mass transfer model proposed properly predicts meat temperature evolution and weight loss during the cooling process after slaughter. The model is validated with experimental data and results from numerical models found in the literature, having a very good concordance despite the uncertainty in beef side geometry, the assumption of uniform thermophysical properties and the simplifications considered in convective heat transfer coefficients.

An upper limit of the meat thickness affected by drying is analytically estimated, resulting in the same order as that obtained by simulation. This analytical estimate is useful for mesh design purposes, but can also be used as an estimate of the affected depth without the need to perform numerical modeling.

Natural convection is relevant, the natural convection coefficients are of the same order of magnitude as the forced ones. Water concentration gradients are not negligible with respect to temperature gradients, so both effects must be considered in natural convection phenomena.

Finally, it is observed that there is a convective coefficient value, assumed constant in the sensitivity analysis, that maximizes weight loss. This is an important result to take into account in order to reduce weight loss. This maximum becomes more relevant when chamber walls temperature is higher. Reducing chamber walls temperature, total weight loss during cooling process is reduced significantly, since it is possible to cool the meat without increasing evaporated mass. This result, from a qualitative study, is interesting and alternatives for the cooling process increasing radiative cooling could be explored in order to reduce weight loss. The radiative cooling applied to meat chilling should be studied in greater depth, and taking into account technological limitations.

6. Appendix: Analysis of boundary layer thickness

Based on the analytical solutions for heat transfer in a semi-infinite solid, an analogue solution could be used for mass transfer, since equations 1 and 2 are analogous. Usually the solution for three simple cases are presented in the bibliograhy [16] always assuming a uniform initial temperature into the solid and different boundary conditions: imposed surface temperature, imposed heat flux, and convective heat transfer with constant fluid temperature and convective heat transfer coefficient. The third case, surface convective heat transfer, appears to be the more adequate to our conditions, however it is important to note that, unlike the thermal case, in equation 15 the variable is not the same on both sides of the equality. On the left hand side the variable is meat water content (liquid) and in the right hand side the variable is surface vapor pressure. Therefore, it is not possible to use the solution of this case for our purposes. The case with imposed surface flux is also not suitable because the mass flow at the surface varies greatly from the beginning of the process to the end. The mass flow can be calculated as in equation 21.

If it is assumed a constant mass flow and equal to the initial one (150.6 g/h m^2) throughout all the process, water content at the surface drops quickly to zero (approximately in 3 hours), which does not represent the real process. If the final mass flow (8.1 g/hm^2) is imposed, the thickness of interest is greatly underestimated. For these reasons, and in order to have an upper bound on the thickness of interest, the solution for imposed surface conce

$$\frac{\rho_l(x,t) - \rho_{l_s}}{\rho_{l_i} - \rho_{l_s}} = erf\left(\frac{x}{2\sqrt{D_m t}}\right) \tag{23}$$

setting an extreme value of $\rho_l(x = 0) = \rho_{l_s} = 0$ and the biggest mass diffusivity, for the initial temperature, using equation 2, D_m =3.15$E - 10$ m/s. The erf is the error function, and $\rho_{l_i} = \rho_l(t = 0)$ is the initial water content set at 834 kg/m^3.

In figure 14 the water content profiles are shown for time zero, 2, 10 and 22 hours. As can be seen the depth penetration δ increases with time. It can be defined as the depth to which significant water content effects propagate within a medium, it is the x position at which, for example, $\frac{\rho_l(x,t)-\rho_{l_s}}{\rho_{l_i}-\rho_{l_s}}$ =0.99. Using equation 23, $\delta_{99\%} = 3.66\sqrt{D_m t}$. It appears to be independent of the surface water content, however it is not real since the 99% is relative to these value and the initial one also, as can be seen in equation 23. For 22 hours the maximum depth penetration is 18 mm. This value is very similar to the one used by Trujillo [10], so it results a good reference.

It is important to note that the value obtained allows to verify the semi infinite solid model assumed, taking into account the beef side dimension. Therefore, it is reasonable to assume an unidirectional diffusion in this layer, since the layer thickness is small respect to curvature ratio.

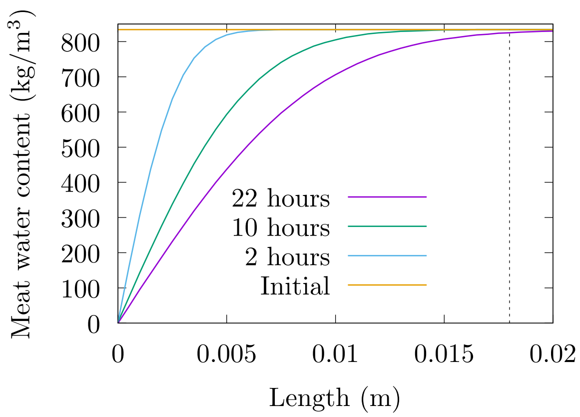

Figure 14: Semi-infinite solid solution for an impose surface water content.

References

[1] F. Toldra, Lawrie´ s Meat Science, 2017.

[2] J. Savell, S. Mueller, B. Baird, The chilling of carcasses, Meat Science 70 (3) (2005) 449–459. doi:10.1016/j.meatsci.2004.06.027.
URL https://linkinghub.elsevier.com/retrieve/pii/S030917400500046X

[3] P.-s. Mirade, A. Kondjoyan, J.-d. Daudin, Three-dimensional CFD calculations for designing large food chillers 34 (2002) 67–88.

[4] K. D. Kuffi, T. Defraeye, B. M. Nicolai, S. De Smet, A. Geeraerd, P. Verboven, CFD modeling of industrial cooling of large beef carcasses, International Journal of Refrigeration 69 (2016) 324–339. doi:10.1016/j.ijrefrig.2016.06.013.
URL http://dx.doi.org/10.1016/j.ijrefrig.2016.06.013https://linkinghub.elsevier.com/retrieve/pii/S014070071630175X

[5] A. Kuitche, J. Daudin, G. Letang, Modelling of temperature and weight loss kinetics during meat chilling for time-variable conditions using an analytical-based method — I. The model and its sensitivity to certain parameters, Journal of Food Engineering 28 (1) (1996) 55–84. doi:10.1016/0260-8774(95)00028-3.

URL https://linkinghub.elsevier.com/retrieve/pii/0260877495000283

[6] P. Mallikarjunan, G. Mittal, Heat and mass transfer during beef carcass chilling — Modelling and simulation, Journal of Food Engineering 23 (3) (1994) 277–292. doi:10.1016/0260-8774(94)90054-X.
URL https://linkinghub.elsevier.com/retrieve/pii/026087749490054X

[7] J. Daudin, A. Kuitche, Modelling of temperature and weight loss kinetics during meat chilling for time variable conditions using an analytical based method — III. Calculations versus measurements on pork carcass hindquarters, Journal of Food Engineering 29 (1) (1996) 39–62. doi:10.1016/0260-8774(95)00063-1.
URL https://linkinghub.elsevier.com/retrieve/pii/0260877495000631

[8] L. Davey, Q. Pham, Predicting the dynamic product heat load and weight loss during beef chilling using a multi-region finite difference approach, International Journal of Refrigeration 20 (7) (1997) 470–482. doi:10.1016/S0140-7007(97)00048-0.
URL https://linkinghub.elsevier.com/retrieve/pii/S0140700799000742https://linkinghub.elsevier.com/retrieve/pii/S0140700797000480

[9] L. Davey, Q. Pham, A multi-layered two-dimensional finite element model to calculate dynamic product heat load and weight loss during beef chilling, International Journal of Refrigeration 23 (6) (2000) 444–456. doi:10.1016/S0140-7007(99)00074-2.
URL https://linkinghub.elsevier.com/retrieve/pii/S0140700799000742

[10] F. J. Trujillo, Q. T. Pham, A computational fluid dynamic model of the heat and moisture transfer during beef chilling, International Journal of Refrigeration 29 (6) (2006) 998–1009. doi:10.1016/j.ijrefrig.2006.05.001.

URL https://linkinghub.elsevier.com/retrieve/pii/S0140700706000892

[11] Lucy Davey, Measurement and Prediction of Product Heat Load and Weight Loss During Beef Chilling, Ph.D. thesis (1998).

[12] Q. Pham, F. Trujillo, N. McPhail, Finite element model for beef chilling using CFD-generated heat transfer coefficients, International Journal of Refrigeration 32 (1) (2009) 102–113. doi:10.1016/j.ijrefrig.2008.04.007.
URL http://dx.doi.org/10.1016/j.ijrefrig.2008.04.007https://linkinghub.elsevier.com/retrieve/pii/S0140700708000790

[13] F. J. Trujillo, C. Wiangkaew, Q. T. Pham, Drying modeling and water diffusivity in beef meat, Journal of Food Engineering 78 (1) (2007) 74–85. doi:10.1016/j.jfoodeng.2005.09.010.
URL https://linkinghub.elsevier.com/retrieve/pii/S0260877405006394

[14] J. Willix, M. B. Harris, J. K. Carson, Local surface heat transfer coefficients on a model beef side 74 (2006) 561–567. doi:10.1016/j.jfoodeng.2005.03.044.

[15] J. F. Cepeda, C. L. Weller, M. Negahban, J. Subbiah, H. Thippareddi, Heat and Mass Transfer Modeling for Microbial Food Safety Applications in the Meat Industry: A Review, Food Engineering Reviews 5 (2) (2013) 57–76. doi:10.1007/s12393-013-9063-6.
URL http://link.springer.com/10.1007/s12393-013-9063-6

[16] A. T.L.Bergman, Fundamentals of heat and mass transfer, 2017.

[17] S. W. Churchill, H. H. S. Chu, Correlating equations for laminar and turbulent free convection from a vertical 18 (1975) 1323–1329.

[18] F. J. Trujillo, P. C. Yeow, Q. Pham, Moisture sorption isotherm of fresh lean beef and external beef fat, Journal of Food Engineering 60 (4) (2003) 357–366. doi:10.1016/S0260-8774(03)00058-X.

URL https://linkinghub.elsevier.com/retrieve/pii/S026087740300058X

[19] D. K. Hoang, S. J. Lovatt, J. R. Olatunji, J. K. Carson, Improved prediction of thermal properties of refrigerated foods, Journal of Food Engineering 297 (January) (2021) 110485. doi:10.1016/j.jfoodeng.2021.110485. URL https://doi.org/10.1016/j.jfoodeng.2021.110485

[20] F. Levy, A modified Maxwell-Eucken equation for calculating the thermal conductivity of two-component solutions or mixtures, International Journal of Refrigeration 4 (4) (1981) 223–225. doi:10.1016/0140-7007(81)90053-0. URL https://linkinghub.elsevier.com/retrieve/pii/0140700781900530

[21] S. J. J. Jame, C., Thermophysical properties of meat, in: Meat refrigeration. Part 3, 2002, Ch. Chapter 13.

[22] D. Lovett, L. Herbert, R. Radford, Carcass chilling-experimental investigation of weight loss from lean meat, International Journal of Refrigeration 1 (1) (1978) 27–32. doi:10.1016/0140-7007(78)90103-2. URL https://linkinghub.elsevier.com/retrieve/pii/0140700778901032